J Membrane Biol (2008) 223:27–36
DOI 10.1007/s00232-008-9110-z

Biochemical Constitution of Extracellular Medium is Critical for Control of Human Breast Cancer MDA-MB-231 Cell Motility

Huiyan Pan · Mustafa B. A. Djamgoz

Received: 22 July 2007 / Accepted: 7 May 2008 / Published online: 25 June 2008

Abstract Although voltage-gated sodium channel (VGSC) activity, upregulated significantly in strongly metastatic human breast cancer cells, has been found to potentiate a variety of in vitro metastatic cell behaviors, the mechanism(s) regulating channel expression/activity is not clear. As a step toward identifying possible serum factors that might be responsible for this, we tested whether medium in which fetal bovine serum (FBS) was substituted with a commercial serum replacement agent (SR-2), comprising insulin and bovine serum albumin, would influence the VGSC-dependent in vitro metastatic cell behaviors. Human breast cancer MDA-MB-231 cells were used as a model. Measurements of lateral motility, transverse migration and adhesion showed consistently that the channel's involvement in metastatic cell behaviors depended on the extracellular biochemical conditions. In normal medium (5% FBS), tetrodotoxin (TTX), a highly specific blocker of VGSCs, suppressed these cellular behaviors, as reported before. In contrast, in SR-2 medium, TTX had opposite effects. However, blocking endogenous insulin/insulin-like growth factor receptor signaling with AG1024 eliminated or reversed the anomalous effects of TTX. Insulin added to serum-free medium increased migration, and TTX increased it further. In conclusion, (1) the biochemical constitution of the extracellular medium had a significant impact upon breast cancer cells' in vitro metastatic behaviors and (2) insulin, in particular, controlled the mode of the functional association between cells' VGSC activity and metastatic machinery.

H. Pan · M. B. A. Djamgoz (✉)
Neuroscience Solutions to Cancer Research Group, Division of Cell and Molecular Biology, Imperial College London, Sir Alexander Fleming Building, South Kensington Campus, London, SW7 2AZ, UK
e-mail: m.djamgoz@imperial.ac.uk

Keywords Serum replacement · Insulin · Tetrodotoxin · Breast cancer · Metastasis · Motility · Adhesion

Introduction

The importance of the chemical constitution of the tumor environment for carcinogenesis and disease progression has frequently been emphasized, more recently in relation to gene expression and stem cells (e.g., Liotta and Kohn 2001; Creighton et al. 2003; Haslam and Woodward 2003; Melillo and Semenze 2006; Postovit et al. 2006; Langley and Fidler 2007; Eccles and Welch 2007; Tysnes and Bjerkvig 2007; Nakamura et al. 2007; Gatenby and Gilles 2008). Furthermore, serum levels of biochemicals are routinely used as cancer markers (e.g., Rodriguez-Pineiro et al. 2006; Boelaert et al. 2006; Tas et al. 2006). In vivo, cancer cells occupy dynamic, interactive surroundings, potentially diverse in their biochemistry and cellular makeup, including reactive stroma and blood vessels (Weigelt, Peterse and van't Veer 2005; Fidler 2003; Tlsty and Coussens 2006). Paget (1889) originally proposed the seminal "seed and soil" hypothesis to explain the non-random patterns of metastases (Witz and Levy-Nissenbaum 2006). The concept that metastasis results from cancer cells interacting with a specific organ microenvironment was formalized by Fidler (2002). Consistent with this, in vitro experiments demonstrated that culture medium is important in determining the cells' membrane characteristics and signaling, including response to pharmacological agents (Kusaka et al. 1998; Lee et al. 2006; Yoshida et al. 2006).

Voltage-gated sodium channels (VGSCs) are expressed commonly in "excitable" cells, such as neurons and muscle cells, as well as in some "nonexcitable" cells, such as lymphocytes and fibroblasts (reviewed in Diss et al. 2004).

There is increasing evidence that upregulation of functional VGSC expression occurs in a variety of human carcinomas of strong metastatic potential, including prostate cancer (Laniado et al. 1997; Bennett et al. 2004), lung cancer (Blandino et al. 1995; Onganer and Djamgoz 2005; Roger et al. 2007), melanoma (Allen et al. 1997; Nilius et al. 1990), breast cancer (BCa) (Roger et al. 2003; Fraser et al. 2005), mesothelioma (Fulgenzi et al. 2006) and cervical cancer (Diaz et al. 2007). In the case of BCa, as in other carcinomas tested, blocking VGSC activity with the highly specific tetrodotoxin (TTX) inhibited a series of in vitro cellular behaviors that would be involved in the metastatic cascade, such as lateral motility, including galvanotaxis, endocytic membrane activity, transverse migration and Matrigel invasion (e.g., Djamgoz et al. 2001; Roger et al. 2003; Fraser et al. 2003, 2005). Similar results were obtained by suppressing the predominant VGSC (neonatal Nav1.5) expression in BCa by small interfering RNA or a polyclonal antibody (Brackenbury et al. 2007). These effects could have clinical relevance since VGSC upregulation has also been seen in vivo: prostate cancer (Diss et al. 2005), small-cell lung cancer (Onganer et al. 2005) and BCa (Fraser et al. 2005).

Although the mechanism(s) responsible for the VGSC upregulation in carcinomas is not known, the biochemical nature of the cellular environment is likely to be important, as in the case of other ion channels and receptors (e.g., Yoshida et al. 2006; Snopko et al. 2007; Zebedin et al. 2007). An earlier study showed that serum concentration indeed had a significant effect on VGSC characteristics in rat prostate cancer cells (Ding and Djamgoz 2004). VGSC expression generally is dynamic and can be modulated by various growth factors, cytokines and hormones (e.g., Diss et al. 2004; Brackenbury and Djamgoz 2006, 2007). In the present study, as a step toward developing experimental conditions for identifying specific VGSC controlling agents, we have investigated the general role of the culture medium on metastatic cell behaviors (MCBs) and their control by VGSC activity in strongly metastatic human BCa MDA-MB-231 cells. As culture conditions, we compared (1) normal medium containing 5% fetal bovine serum (FBS) with (2) medium in which FBS was substituted with a commercial "serum replacement–2" (SR-2) agent. As MCBs, lateral motility, transverse migration and single-cell adhesion were studied.

Materials and Methods

Cell Culture

MDA-MB-231 cells were grown routinely in Dulbecco's modified Eagle medium (DMEM), supplemented with 4 mM L-glutamine and 5% FBS (Fraser et al. 2005). For general maintenance, the cells were plated at a density of approximately 10^5 in a 10-cm-diameter tissue culture dish with 6 ml of medium. After 24 h of plating and equilibration, the medium was changed to one containing (1) 5% FBS (control) or (2) SR-2 agent, which contains mainly insulin and bovine serum albumin (BSA). SR-2 agent was prepared according to the manufacturer's instructions (Sigma, St. Louis, MO).

Pharmacological Agents

TTX (Alomone Labs, Jerusalem, Israel), stored as a stock solution (3,132 μM) in culture medium at −20°C, was defrosted and diluted as required. AG1024 (Sigma), an inhibitor of insulin/insulin-like growth factor receptor (Parrizas et al. 1997; Deutsch et al. 2004), was made up as a stock solution (3,277 μM) in dimethyl sulfoxide (DMSO) and diluted in the appropriate medium to give the required working concentration (0.1–5.0 μM). The final concentration of DMSO was 0.01–0.1%. Human insulin (Sigma) was diluted in serum-free DMEM and used at a working concentration of 100 nM.

MCB Assays

A number of functional assays were performed, as follows. Similar results were obtained from cells treated pharmacologically for 24 or 48 h. In the text, data are given mainly for 24-h treatments.

Lateral Motility

Lateral motility was assessed by a monolayer wound-heal assay (Fraser et al. 2003). On day 1, cells were plated at a density of 5×10^5/dish and allowed to settle for 24 h. On day 2, "wounds" of 0.6–0.9 mm width were created. For cells in 5% FBS, 10 μM TTX (in 5% FBS) was added to each dish. Wound widths were determined immediately afterward (0 h) by measuring at the 45 fixed intersection points in each dish. The same sites were remeasured 24 and 48 h afterward, with a change of medium with the same in between. For experiments involving SR-2 medium, FBS was replaced with SR-2 agent on day 2 and the cells were allowed to reequilibrate for 24 h. On day 3, TTX (10 μM) was applied to the cells in SR-2 medium and the assays continued as above. Each treatment had its respective control at all times and was repeated at least three times, thus giving at least 405 individual data points for each condition. Lateral motility was quantified as "motility index" (MoI), defined as follows:

$$\mathrm{MoI} = 1 - (W_t/W_0)$$

where W_0 is the initial wound width and Wt is the width of the wound at time t (24 or 48 h).

Transverse Migration

Polycarbon "Transwell" membrane filters of 12-μm pore size (Corning Costar, Cambridge, MA) were inserted in 12-well plates. Initial plating density was 2×10^5 cells/well, and the pharmacological treatment strategy was as above, involving (1) TTX (10 μM), (2) AG1024 (0.5 μM) or (3) AG1024 (0.5 μM) + TTX (10 μM) and added to the upper and lower chambers. In a further experiment, 0.1% BSA in serum-free DMEM was used as a basal medium to study migration. Following initial plating/conditioning in 5% FBS and then in 0.1% BSA (24 h each), cells (2×10^5/well) were treated with (1) TTX (10 μM), (2) insulin (100 nM) or (3) insulin (100 nM) + TTX (10 μM), while the lower chamber was filled with 1 ml of 1% FBS medium supplemented with corresponding drug(s). In each experiment, after 8 h of treatment during the assay, the medium was removed from both chambers and all the cells in the top chamber were scraped with swabs. The number of migrated cells was determined using the MTT method (Fraser et al. 2005; van de Loosdrecht et al. 1994). Migration index (MiI) was defined as follows:

$$\mathrm{MiI}(\%) = (N_m/N_0) \times 100$$

where N_m is the number of migrated cells and N_0 is the original cell number.

Adhesion

A recently devised "single-cell adhesion measurement apparatus" (SCAMA) was used (Palmer et al. 2008). Suction was applied to individual cells via a glass micropipette (tip sizes 19–22 μm o.d.). The detachment negative pressure (DNP) was recorded on-line using a digital manometer. Drug treatment regimes were as above. The following drugs were tested: (1) TTX (10 μM), (2) AG1024 (0.5 μM) and (3) AG1024 (0.5 μM) + TTX (10 μM). For each condition, at least 30 healthy-looking single cells were selected for the adhesion measurements, and cell size was determined from the average of longest and shortest diameters. Each treatment was evaluated from at least three separate experiments, each performed in triplicate. The average value of the DNP relative to the cell size (DNPR) was calculated as follows:

$$\mathrm{DNPR}\ (\mathrm{kPa}/\mu\mathrm{m}^2) = \mathrm{DNP}\ (\mathrm{kPa})/\mathrm{cell\ size}(\mu\mathrm{m}^2)$$

Proliferation and Toxicity

Proliferation and toxicity assays have been described in detail by Fraser et al. (1999). The pharmacological treatment regimes were as above.

Western Blotting

Cells reconditioned in 0.1% BSA for 24 h were treated with insulin (100 nM) for 48 h and then lysed in radioimmunoprecipitation buffer with a 1:100 dilution of protease inhibitor mixture (Sigma). Protein yield was determined using a Bradford dye binding assay (Bio-Rad, Richmond, CA). Samples (60 μg) of protein from different lysates were resolved against a wide-range color/size marker (Sigma) by 6% sodium dodecyl sulfate polyacrylamide gel electrophoresis (Chioni et al. 2005). Proteins were transferred to a nitrocellulose membrane at 4°C in a buffer containing 25 nM Tris and 192 mM glycine and run at 30 *V* overnight. Nitrocellulose membranes were blocked for 1 h in 5% (w/v) nonfat dried milk/phosphate-buffered saline (PBS), followed by a 30-min wash in 2% (w/v) BSA/PBS. Two primary antibodies were used, diluted in 2% (w/v) BSA/PBS, to final concentrations, as follows: (1) pan-VGSC antibody (1 μg/ml; Upstate Biotechnology, Buckingham, UK) and (2) anti-actinin antibody (1 μl/ml, Sigma). The secondary antibodies were peroxidase-conjugated swine-antirabbit, and goat-antimouse (Dako, Glostrup, Denmark) for (1) and (2), respectively. Blots were developed using the enhanced chemiluminescence system (Amersham, Aylesbury, UK) and visualized by exposure to Super RX 100NF film (Fuji, Tokyo, Japan). Densitometric analysis was performed using Image-Pro Plus software (Media Cybernetics, Silver Spring, MD). Band densities were normalized to anti-actinin as loading control and averaged from at least three separate treatments.

Immunocytochemistry and Confocal Microscopy

Cells (5×10^4) were plated onto poly-L-lysine-coated coverslips in 24-well plates in 5% FBS. On day 2, the medium was changed to serum-free medium but with added 0.1% BSA for 24 h. On days 3 and 4, insulin (100 nM) was applied to the cells with a medium change with the same in between. On day 5, the cells were fixed in 4% (w/v) paraformaldehyde/PBS for 15 min. Cells were labeled first with 0.2 mg/ml fluorescein isothiocyanate (FITC)–conjugated concanavalin A (Sigma) in 5% BSA/PBS for 30 min as a plasma membrane marker, then permeabilized for 10 min with 0.1% (w/v) saponin at room temperature. Nonspecific binding sites were blocked for 1 h with 5% BSA/PBS, and then the cells were incubated with the primary antibody (pan-VGSC, 1:100) for 1 h, followed by the Alexa567-conjugated goat antirabbit secondary antibody (1:100, Dako) for 1 h. Finally, cells were washed in distilled H_2O and mounted in Vectashield antifading mounting medium (Vector, Burlingame, CA).

Cells were examined on a Leica (Cambridge, UK) DM IRBE microscope with a confocal laser scanner (Leica TCS-NT). FITC and/or Alexa567 were excited with the 488 and 568 nm laser lines, respectively. The images were captured simultaneously from the two channels using a confocal pinhole of 226.9 μm (Airy 1).

Digital analysis was performed using LCS Lite software (Leica), as follows (Brackenbury and Djamgoz 2006):

1. Cell surface protein level was initially quantified using the "freeform line profile" function drawn around the cell periphery, judged by conconavalin A staining. Measurements were taken from 20–30 cells (randomly chosen) per condition for three repeat treatments.
2. The subcellular distribution of VGSC protein was determined using the "straight line profile" function drawn across the cytoplasm avoiding the nucleus. Signal intensity in the plasma membrane region, set to cover 1.5 μm inward from the edge of concanavalin A staining, was compared with cytoplasmic signal intensity within the central 30% of the line profile. Measurements were taken from eight or more cells (randomly chosen) per condition for three repeat treatments.

Data Analysis

All data were calculated as means ± standard error of the mean (SEM). Statistical comparisons between data sets were performed using Student's *t*-test or analysis of variance, followed by Newman-Keuls post hoc analyses, as appropriate. Differences were considered statistically significant at $P < 0.05$.

Results

Initial Observations

MDA-MB-231 cells incubated in normal 5% FBS medium were round and refractive (Fig. 1A). In contrast, MDA-MB-231 cells grown in SR-2 medium appeared flat and most had extended pseudopodia (Fig. 1B). Proliferation of MDA-MB-231 cells was greater by 25 ± 4% in 5% FBS vs. SR-2 medium ($P < 0.05$, $n = 4$). At the working concentrations used, neither TTX (10 μM) nor AG1024 (0.5 μM) had any effect on proliferation in either medium over 48 h. Cell viability also was not affected by treating the cells with either 10 μM TTX or 5 μM AG1024. In the following, we describe results on cellular lateral motility, transverse migration and adhesion as key examples of MCB.

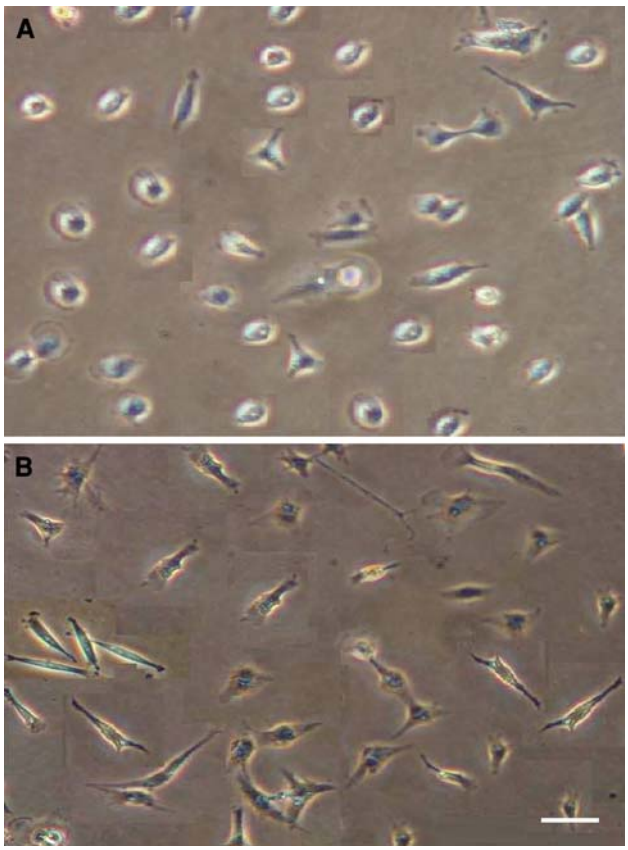

Fig. 1 Phase-contrast photomicrographs of MDA-MB-231 cells grown in normal (5% FBS) (**A**) and SR-2 (**B**) media for 48 h. The cells were plated at an initial density of 5×10^4 per dish in FBS, and the medium was changed as described in "Materials and Methods." Cells were photographed "live." Scale bar = 20 μm (**A**, **B**)

Effects of TTX on MDA-MB-231 Cells in FBS and SR-2 Media

Cellular motility was quantified by two different, complementary methods and analyzed as follows.

The value of MoI (determined from lateral motility assays) was 21% higher in 5% FBS compared with SR-2 medium ($P < 0.05$, $n = 4$; Fig. 2A). Treatment with TTX (10 μM) reduced motility in 5% FBS medium by 9.4 ± 2.1% after 24 h ($P < 0.05$, $n = 4$; Fig. 2A). In contrast, for cells grown in SR-2 medium, similar treatment with TTX increased motility by 33 ± 3.1% ($P < 0.05$, $n = 4$; Fig. 2A).

Transverse migration of MDA-MB-231 cells was studied using Transwell assays, which excluded any effect on proliferation. Similar to lateral motility, MiI of MDA-MB-231 cells grown in 5% FBS was significantly (32 ± 4.2%) higher than that for the SR-2 medium ($P < 0.05$, $n = 4$; Fig. 2B). In 5% FBS medium, TTX (10 μM) significantly reduced MiI by 32 ± 4.6%, from 3.1 ± 0.3% to 2.1 ± 0.3% ($P < 0.05$, $n = 4$; Fig. 2B). In contrast, in SR-2

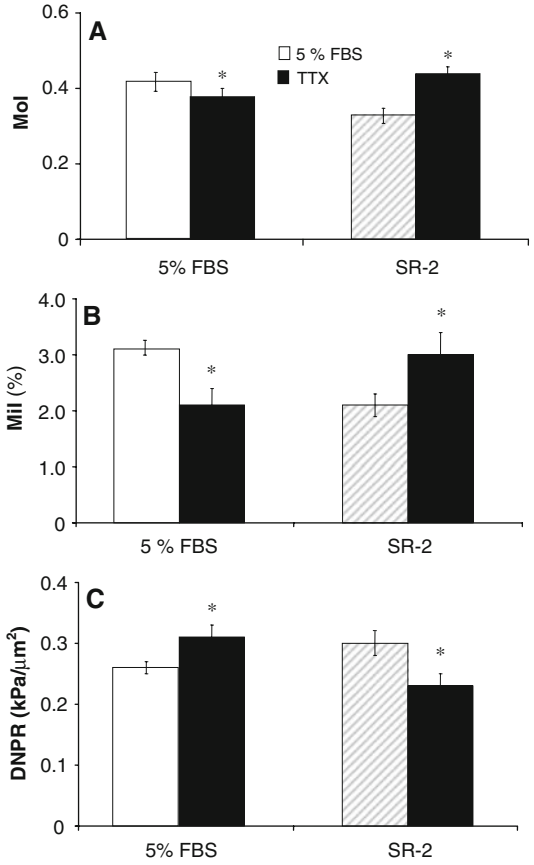

Fig. 2 Effects of TTX on metastatic behavior of MDA-MB-231 cells grown in normal (5% FBS) and SR-2 media after 24 h. (**A**) Lateral motility, quantified as MoI. *White bars*, Control data obtained from cells in 5% FBS and SR-2 media. *Black bars*, Data obtained from 10 μM TTX–treated cells in two different media. (**B**) Transwell migration data (quantified as MiI) plotted as in (**A**). (**C**) Single-cell adhesion (quantified as DNPR), also plotted as in (**A**). Each histobar represents mean ± standard error. *Statistically significant difference at $P < 0.05$ (compared with the respective, adjacent control). Inset in (**A**) applicable to all parts

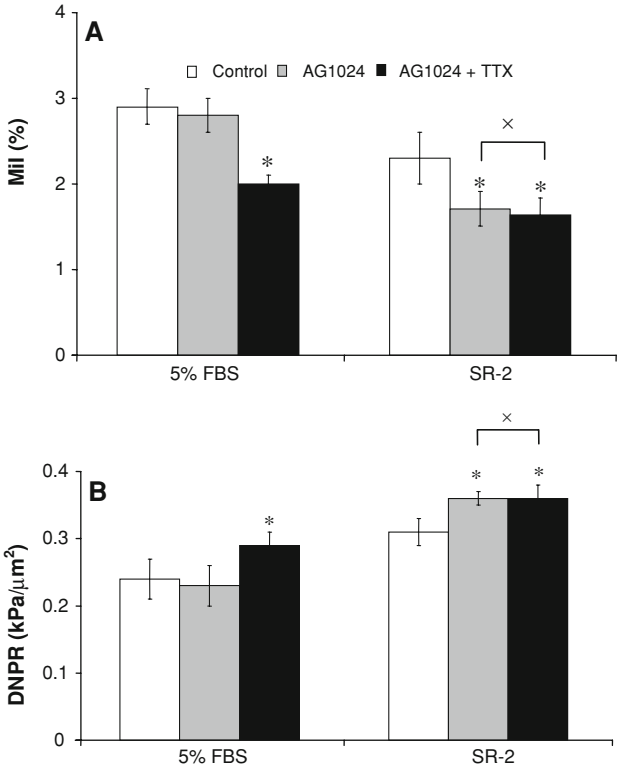

Fig. 3 Effects of AG1024, TTX and combinations on transverse migration (MiI) and single-cell adhesion (DNPR) of MDA-MB-231 cells after 24-h treatments. (**A**) Effects of AG1024 (0.5 μM) and AG1024 + TTX (10 μM) on MiI of cells grown in 5% FBS and SR-2 media. (**B**) As in (**A**), on single-cell adhesion (DNPR). Each histobar represents mean ± standard error. *Statistically significant difference at $P < 0.05$ (compared with the respective, adjacent control). [x]No statistically significant difference. Inset in (**A**) applicable to both parts

medium, TTX (10 μM) significantly increased MiI by 40 ± 3.3%, from 2.1 ± 0.2% to 3.0 ± 0.4% ($P < 0.05$, $n = 7$; Fig. 2B).

The average values of DNPR for MDA-MB-231 cells grown in 5% FBS medium and SR-2 medium were 0.26 ± 0.02 and 0.30 ± 0.04 kPa/μm^2, respectively (Fig. 2C). Thus, again, cellular adhesion was higher in the SR-2 medium by 15% ($P < 0.05$, $n = 4$). In 5% FBS, TTX increased adhesion by 23%, the DNPR value rising from 0.26 ± 0.01 to 0.32 ± 0.02 kPa/μm^2 after 24 h ($P < 0.05$, $n = 4$). In contrast, TTX reduced the adhesion of cells in SR-2 medium by 23%, from 0.30 ± 0.02 to 0.23 ± 0.02 kPa/μm^2 ($p < 0.05$, $n = 4$; Fig. 2C).

This set of experiments led to two main conclusions: (1) MDA-MB-231 cell MCBs were less pronounced in SR-2 medium–i.e., lateral motility and transverse migration were reduced, while adhesion increased–and (2) TTX had opposite effects on MCBs when cells were incubated in 5% FBS vs. SR-2 medium. The effects of TTX in 5% FBS were as reported before (Fraser et al. 2005; Brackenbury et al. 2007), consistent with VGSC activity enhancing MCBs. However, the involvement of VGSC activity in the control of MCB was reversed in SR-2 medium.

Possible Cause of the Anomalous (Reversed) VGSC Effect

Since the main active component of the SR-2 agent is insulin, we next investigated whether this could be responsible for the anomalous effects of TTX.

Endogenous Insulin

Addition of AG1024 (0.5 μM), an inhibitor of insulin receptor tyrosine kinase, to 5% FBS had no effect on the migration of MDA-MB-231 cells: MiI = 2.9 ± 0.2% (control) and 2.8 ± 0.2% (AG1024-treated) ($P > 0.05$, $n = 5$; Fig. 3A). Furthermore, in the presence of AG1024,

TTX (10 μM) still decreased migration by 31 ± 5%, from 2.9 ± 0.20% to 2.0 ± 0.16% ($P < 0.05$ vs. control, $n = 5$; Fig. 3A). In contrast, addition of AG1024 to SR-2 medium significantly decreased migration (Fig. 3A); this effect was dose-dependent (not shown), reaching 49 ± 6% inhibition for 1 μM AG1024. Cotreatment with AG1024 (0.5 μM) + TTX (10 μM) also reduced migration by 28 ± 6%, from 2.3 ± 0.19% to 1.6 ± 0.24% (Fig. 3A). There was no difference between the effect of the co-treatment and equimolar AG1024 alone (27 ± 5% reduction; $P > 0.05$, $n = 5$). There was a similar effect of AG1024 on adhesion (Fig. 3B). In 5% FBS medium, AG1024 (0.5 μM) alone had no effect ($P > 0.05$, $n = 5$) and AG1024 (0.5 μM) + TTX (10 μM) significantly increased adhesion of the cells by 20 ± 3% ($P < 0.05$, $n = 5$). In contrast, in SR-2 medium, both AG1024 (0.5 μM) alone and coapplication with TTX (10 μM) significantly increased cell adhesion (Fig. 3B). When treated with AG1024 alone, DNPR increased by 19 ± 4% ($P < 0.05$, $n = 5$). Coapplication with TTX (10 μM) increased DNPR by 21 ± 3% ($P < 0.05$, $n = 5$); there was no difference in the effects of TTX and TTX + AG1024 ($P > 0.05$, Fig. 3B). Thus, the anomalous effects of TTX on migration and adhesion in SR-2 medium were blocked in the presence of AG1024.

Exogenous Insulin

Further experiments were carried out on MDA-MB-231 cells in basal serum-free medium with added 0.1% BSA (Fig. 4). In this medium, TTX decreased migration significantly, as in normal FBS medium. Application of exogenous insulin (100 nM) in BSA medium increased migration by 44% ($P < 0.05$, $n = 6$). TTX (10 μM) coapplied with insulin (100 nM) further increased MiI by 35%

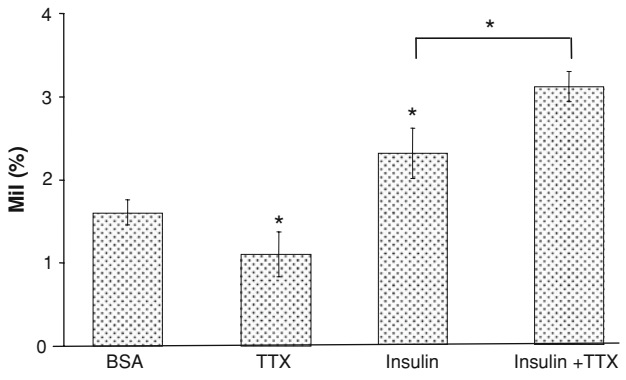

Fig. 4 Effects of exogenous insulin (100 nM) ± TTX (10 μM) on transverse migration (MiI) of MDA-MB-231 cells. The control solution contained 0.1% BSA added to DMEM (no serum present). Each histobar represents mean ± standard error. *Statistically significant difference at $P < 0.05$ (compared with the respective, adjacent control)

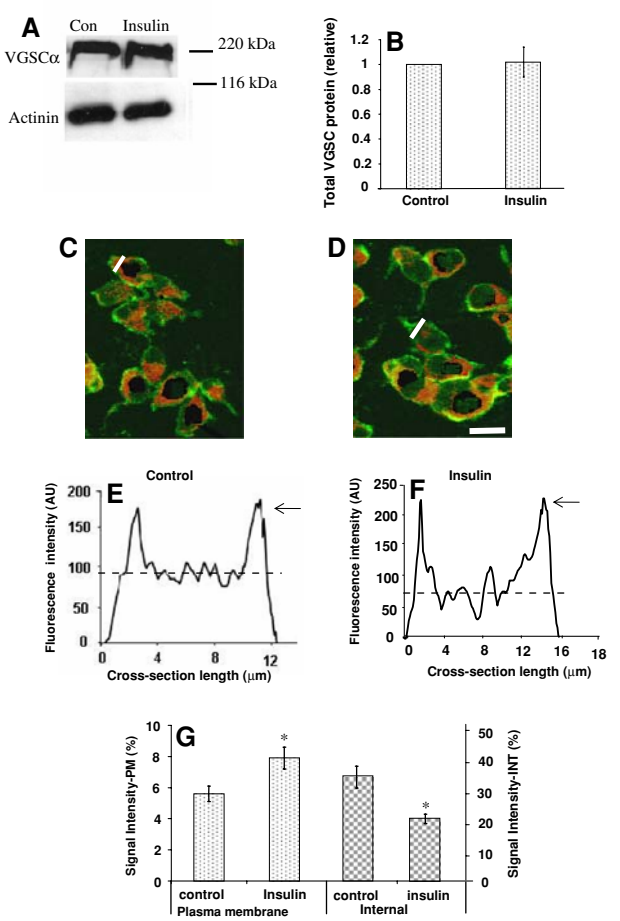

Fig. 5 Effects of exogenous insulin (100 nM, applied for 24 h) on total and subcellular distribution of VGSC protein levels. (**A**) Western blot with pan-VGSC and actinin antibodies. (**B**) Relative levels of total VGSC protein (from **A**), normalized to the actinin control. Typical confocal images of control cells (**C**) and cells treated with insulin for 48 h (**D**), double-labeled with pan-VGSC antibody (red) and concanavalin A plasma membrane marker (green). Scale bar in (**D**) = 15 μm (applicable to both images shown). *Short white bars* indicate examples of cross-sectional images taken. (**E, F**) Profile of digital images of subcellular VGSC immunofluorescence of control (**E**) and insulin-treated (**F**) cells. AU, arbitrary unit. *Arrows*, plasma membrane level; *dotted lines*, cytosolic levels (both drawn by eye). (**G**) Summary of data from (**E**) and (**F**) analyzed as described in "Materials and Methods." PM, plasma membrane; INT, internal fraction. Quantitative data are presented in (**B**) and (**G**) as means ± SEM. *Statistically significant difference at $P < 0.05$ (compared with the respective, adjacent control)

($P < 0.05$ vs. TTX alone, $n = 6$; Fig. 4). In conclusion, (1) insulin enhanced MCBs, (2) the contribution of VGSC activity to MCB enhancement was reversed in insulin-containing media (i.e., SR-2 medium or BSA + insulin medium) and (3) blocking endogenous insulin receptor activity in SR-2 medium eliminated the VGSC role. These data, taken together, suggest that insulin could upregulate functional VGSC expression. This possibility was investigated as follows.

Effect of Insulin on VGSC Protein Expression

Western blot with a pan-VGSC α-subunit antibody revealed that treatment with insulin (100 nM) for up to 48 h did not affect the total VGSC protein level (Fig. 5A, B). However, quantification of peripheral VGSC expression by the freeform line profile analysis suggested that insulin caused a 38% increase in the plasma membrane VGSC level ($P < 0.05$, $n = 70$). Confocal immunocytochemistry and digital image analysis were used also to assess the effect of insulin on the subcellular distribution of VGSC protein. The profile of VGSC immunoreactivity along the cell cross section changed following insulin treatment (Fig. 5C–G). Again, insulin increased the level of VGSC protein in the plasma membrane region by some 41%, from 5.6 ± 0.8% to 7.9 ± 0.9% of total cross-sectional immunofluorescence ($P < 0.05$, $n = 25$ for each; Fig. 5G). There was an opposite effect on the intracellular region: Insulin decreased it by some 39%, the VGSC immunofluorescence falling from 36.5 ± 2.0% to 22.2 ± 0.6% ($P < 0.05$, $n = 25$; Fig. 5G). It was concluded that insulin upregulated VGSC expression in the plasma membrane by changing the balance of the protein recycling in favor of externalization.

Discussion

In summary, the following results were obtained for the MDA-MB-231 cell model of metastatic BCa. (1) The cells' morphology and MCBs (lateral motility, transverse migration and adhesion) were indicative of a more metastatic (including proliferative) state in FBS compared with SR-2 medium. (2) VGSC activity enhanced MCBs in 5% FBS medium but was inhibitory in SR-2 medium. (3) Inhibiting endogenous insulin receptor activity blocked the VGSC effects in SR-2 medium. In medium containing exogenous insulin, again, the role of VGSC was reversed. These results were consistent with insulin being the main cause of the anomalous (reversed) involvement of VGSC activity in control of MDA-MB-231 cells' metastatic behavior (lateral motility, transverse migration and adhesion) in SR-2 medium. (4) Application of insulin in BSA medium increased cellular migration and concurrently induced externalization of VGSC protein. Overall, these results supported the general notion that MCB and its control are influenced critically by the chemical constitution of the cellular environment.

Possible Effects of Insulin on VGSC

Insulin has long been known to exert pleiotropic effects on the development and maintenance of the nervous system by regulating expression of various genes, including VGSCs (e.g., de Pablo and de la Rosa 1995; Yamamoto et al. 1996). Our study showed that insulin could have a significant effect upon the VGSC control of MCBs in MDA-MB-231 cells, which possess insulin receptors (Papa et al. 1997; Zhang et al. 2007). In SR-2 medium (insulin + BSA), VGSC activity decreased migration; this effect was lost after blocking endogenous insulin receptor activity. Similarly, in serum-free medium with 0.1% BSA, insulin increased migration and insulin + TTX increased it further. This suggested a possible interdependence of insulin and VGSC activity. Previous studies have shown that insulin may play a role in regulating functional VGSC expression. Insulin upregulated VGSC expression in bovine adrenal chromaffin cells by enhancing membrane trafficking/protein synthesis rather than increasing the VGSCα mRNA level (Yamamoto et al. 1996; Wada et al. 2004). Insulin also facilitated the induction of Na^+ channels in plasma membrane of *Xenopus laevis* oocytes (Charpentier 2005). It is not known if insulin-induced phosphorylation might also be a factor (Ahern et al. 2005; Hirose et al. 2004). The fact that TTX had no effect on MCBs in the presence of AG1024 would imply that, in addition, insulin could reduce the coupling of VGSC to the MCB machinery (Fig. 6). Such a secondary effect could involve the cytoskeleton, which is well known to be modulated by insulin (e.g., Berfield et al. 1997; Tobe et al. 2003; Berres et al. 2006). Furthermore, Nav1.5, the predominant VGSC (neonatal splice variant) present in MDA-MB-231 cells, is likely to be associated with a range of cytoskeletal elements (Ou et al. 2003; Herfst et al. 2004; D. Shao, K. Okuse and M. B. A. Djamgoz, unpublished data).

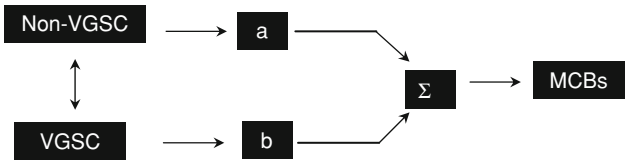

Fig. 6 A conceptual scheme for control of MCBs by VGSC-dependent and non-VGSC mechanisms. In this model, we assume that basal control of MCBs occurs via conventional mechanisms not involving VGSC activity. However, acquisition of strong metastatic potential by the cells is accompanied by VGSC expression, and the two control mechanisms summate (indicated by Σ) to enhance MCBs. *a* and *b* indicate couplers that connect the control mechanisms to the MCB machinery. Importantly, VGSC-dependent and non-VGSC mechanisms can interact (indicated by *two-way arrow*)

Control of Cellular Migration by VGSC Activity

VGSC upregulation occurs in strongly metastatic cells of human BCa (Roger et al. 2003; Fraser et al. 2005). Invasiveness of MDA-MB-231 cells was potentiated by VGSC activity, and a reduction of 30–49% was observed after

treatment with TTX in 5% FBS; Transwell migration was reduced by 52% (Roger et al. 2003; Fraser et al. 2005). The present findings on MDA-MB-231 human BCa cells bathed in normal (5% FBS) medium are in general agreement with these data. On the other hand, in the presence of insulin, the contribution of VGSC activity to MCBs reversed and TTX increased migration. Thus, it would appear that VGSC activity can accelerate or decelerate migration, depending upon the chemical environment of the metastasizing cell. Such dual control would constitute a servo system appropriate for the highly regulated and dynamic nature of the metastatic cascade. Developing neurons were also shown to possess such a characteristic (Guan et al. 2007), and it has been noted that cancer cell invasion has some of the hallmarks of normal neuronal development (Liotta and Clair, 2000).

The mechanisms of VGSC involvement in cellular motility/cytoskeleton broadly could be as follows (Mycielska and Djamgoz 2004).

Direct

Nav1.5 is one of only two VGSCs that has PDZ domains that could enable cytoskeletal interactions (Gavillet et al. 2006). Some 28 proteins were identified as associated with the VGSC (Nav1.8) intracellular domain, including actin and inositol polyphosphate 5-phosphatase (Malik-Hall et al. 2003; Ratcliffe et al. 2000). It is also possible that VGSC β-subunit(s) facilitates VGSC–cytoskeleton and VGSC–extracellular matrix interactions (Isom 2002), and ankyrin may also participate (Komada and Soriano 2002).

Indirect

Indirect effects could occur via ionic changes. For example, Na^+ influx through VGSCs could increase the intracellular Ca^{2+} concentration locally by inhibiting or even reversing Na^+ –Ca^{2+} exchange (Lemos et al. 2007) and/or by altering the release/uptake of Ca^{2+} from intracellular stores by deregulation of intracellular pH (Ishibashi et al. 1999). Furthermore, the rise in intracellular Na^+ influx could activate a variety of enzymes, such as Na^+/K^+ -ATPase (Page and Di Cera 2006) and adenylate cyclase/protein kinase A (Cooper et al. 1998; Brackenbury and Djamgoz 2006); in particular, protein kinase A activation may, in turn, lead to phosphorylation of cytoskeletal components (e.g., Han and Rubin 1996; Liu et al. 2001).

Conclusions

MCBs of MDA-MB-231 cells and the mode of their control by VGSC activity were found to be influenced significantly by the biochemical constitution of the cellular environment. In this regard alone, therefore, extreme care must be taken in adopting commercially available agents for serum replacement. Insulin could have a significant effect on VGSC expression/activity and the consequent control of MCBs. Further work is required to elucidate how these results might relate to the pathophysiological role and clinical potential of insulin/insulin-like growth factor in BCa (e.g., Frasca et al. 2003; Perks and Holly 2003; Zhang and Yee 2004).

Acknowledgement This study was supported by an Amber Fellowship (PCRF) to H. P.

References

Ahern CA, Zhang JF, Wookalis MJ, Horn R (2005) Modulation of the cardiac sodium channel Nav1.5 by Fyn, a Src family tyrosine kinase. Circ Res 96:991–998

Allen DH, Lepple-Wienhues A, Cahalan MD (1997) Ion channel phenotype of melanoma cell lines. J Membr Biol 155:27–34

Bennett ES, Smith BA, Harper JM (2004) Voltage-gated Na^+ channels confer invasive properties on human prostate cancer cells. Pfluegers Arch 447:908–914

Berfield AK, Spicer D, Abrass CK (1997) Insulin-like growth factor I (IGF-I) induces unique effects in the cytoskeleton of cultured rat glomerular mesangial cells. J Histochem 45:583–593

Berres R, Gremeaux T, Gual P, Gonzales T, Gugenheim J, Tran A, Le Marchand-Brustel Y, Tanti JF (2006) Enigma interacts with adaptor protein with PH and SH2 domains to control insulin-induced actin cytoskeleton remodelling and glucose transporter 4 translocation. Mol Endocrinol 20:2864–2875

Blandino JK, Viglione MP, Bradley WA, Oie HK, Kim YI (1995) Voltage-dependent sodium channels in human small-cell lung cancer cells: role in action potentials and inhibition by Lambert-Eaton syndrome IgG. J Membr Biol 143:153–163

Boelaert K, Horacek J, Holder RL, Watkinson JC, Sheppard MC, Franklyn JA (2006) Serum thyrotropin concentration as a novel predictor of malignancy in thyroid nodules investigated by fine-needle aspiration. J Clin Endocrinol Metab 91:4295–4301

Brackenbury WJ, Djamgoz MBA (2006) Activity-dependent regulation of voltage-gated Na^+ channel expression in Mat-LyLu rat prostate cancer cell line. J Physiol 573:343–356

Brackenbury WJ, Djamgoz MBA (2007) Nerve growth factor enhances voltage-gated Na^+ channel activity and Transwell migration in Mat-LyLu rat prostate cancer cell line. J Cell Physiol 210:602–608

Brackenbury WJ, Chioni AM, Diss JK, Djamgoz MBA (2007) The neonatal splice variant of Nav1.5 potentiates in vitro invasive behavior of MDA-MB-231 human breast cancer cells. Breast Cancer Res Treat 101:149–160

Charpentier G (2005) Insulin facilitates the induction of the slow Na^+ channels in immature *Xenopus* oocytes. Gen Physiol Biophys 24:57–73

Chioni AM, Fraser SP, Pani F, Foran P, Wilkin GP, Diss JK, Djamgoz MBA (2005) A novel polyclonal antibody specific for the Nav1.5 voltage-gated Na^+ channel "neonatal" splice form. J Neurosci Methods 147:88–98

Cooper DM, Schell MJ, Thorn P, Irvine RF (1998) Regulation of adenylyl cyclase by membrane potential. J Biol Chem 273:27703–27707

Creighton C, Kuick R, Misek DE, Rickman DS, Brichory FM, Rouillard JM, Omenn GS, Hanash S (2003) Profiling of pathway-specific changes in gene expression following growth of human cancer cell lines transplanted into mice. Genome Biol 4:R46

de Pablo F, de la Rosa EJ (1995) The developing CNS: a scenario for the action of proinsulin, insulin and insulin-like growth factors. Trends Neurosci 18:143–150

Deutsch E, Maggiorella L, Wen B, Bonnet ML, Khanfir K, Frascogna V, Turhan AG, Bourhis J (2004) Tyrosine kinase inhibitor AG1024 exerts antileukaemic effects on STI571-resistant Bcr-Abl expressing cells and decreases AKT phosphorylation. Br J Cancer 91:1735–1741

Diaz D, Delgadillo DM, Hernandez-Gallegos E, Ramirez-Dominguez ME, Hinojosa LM, Ortiz CS, Berumen J, Camacho J, Gomora JC (2007) Functional expression of voltage-gated sodium channels in primary cultures of human cervical cancer. J Cell Physiol 210:469–478

Ding Y, Djamgoz MB (2004) Serum concentration modifies amplitude and kinetics of voltage-gated Na^+ current in the Mat-LyLu cell line of rat prostate cancer. Int J Biochem Cell Biol 36:1249–1260

Diss JK, Fraser SP, Djamgoz MBA (2004) Voltage-gated Na^+ channels: multiplicity of expression, plasticity, functional implications and pathophysiological aspects. Eur Biophys J 33:180–193

Diss JK, Stewart D, Pani F, Foster CS, Walker MM, Patel A, Djamgoz MBA (2005) A potential novel marker for human prostate cancer: voltage-gated sodium channel expression in vivo. Prostate Cancer Prostatic Dis 8:266–273

Djamgoz MBA, Mycielska M, Madeja Z, Fraser SP, Korohoda W (2001) Directional movement of rat prostate cancer cells in direct-current electric field: involvement of voltage-gated Na^+ channel activity. J Cell Sci 114:2697–2705

Eccles SA, Welch DR (2007) Metastasis: recent discoveries and novel treatment strategies. Lancet 369:1742–1757

Fidler IJ (2002) The organ microenvironment and cancer metastasis. Differentiation 70:498–505

Fidler IJ (2003) The pathogenesis of cancer metastasis: the "seed and soil" hypothesis revisited. Nat Rev Cancer 3:453–458

Frasca F, Pandini G, Vigneri R, Goldfine ID (2003) Insulin and insulin/IGF receptors are major regulators of breast cancer cells. Breast Dis 17:73–89

Fraser SP, Ding Y, Liu A, Foster CS, Djamgoz MBA (1999) Tetrodotoxin suppresses morphological enhancement of the metastatic MAT-LyLu rat prostate cancer cell line. Cell Tissue Res 295:505–512

Fraser SP, Diss JK, Chioni AM, Mycielska ME, Pan H, Yamaci RF, Pani F, Siwy Z, Krasowska M, Grzywna Z, Brackenbury WJ, Theodorou D, Koyuturk M, Kaya H, Battaloglu E, De Bella MT, Slade MJ, Tolhurst R, Palmieri C, Jiang J, Latchman DS, Coombes RC, Djamgoz MBA (2005) Voltage-gated sodium channel expression and potentiation of human breast cancer metastasis. Clin Cancer Res 11:5381–5389

Fraser SP, Salvador V, Manning EA, Mizal J, Altun S, Raza M, Berridge RJ, Djamgoz MBA (2003) Contribution of functional voltage-gated Na^+ channel expression to cell behaviors involved in the metastatic cascade in rat prostate cancer: I lateral motility. J Cell Physiol 195:479–487

Fulgenzi G, Graciotti L, Faronato M, Soldovieri MV, Miceli F, Amoroso S, Annunziato L, Procopio A, Taglialatela M (2006) Human neoplastic mesothelial cells express voltage-gated sodium channels involved in cell motility. Int J Biochem Cell Biol 38:1146–1159

Gatenby RA, Gilles RJ (2008) A microenvironmental model of carcinogenesis. Nat Rev Cancer 8:56–61

Gavillet B, Rougier JS, Domenighetti AA, Behar R, Boixel C, Ruchat P, Lehr HA, Pedrazzini T, Abriel H (2006) Cardiac sodium channel Nav1.5 is regulated by a multiprotein complex composed of syntrophins and dystrophin. Circ Res 99:407–414

Guan CB, Xu HT, Jin M, Yuan XB, Poo MM (2007) Long-range Ca^{2+} signalling from growth cone to soma mediates reversal of neuronal migration induced by Slit-2. Cell 129:385–395

Han JD, Rubin CS (1996) Regulation of cytoskeleton organization and paxillin dephosphorylation by cAMP studies on murine Y1 adrenal cells. J Biol Chem 271:29211–29215

Haslam SZ, Woodward TL (2003) Host microenvironment in breast cancer development: epithelial-cell–stromal-cell interactions and steroid hormone action in normal and cancerous mammary gland. Breast Cancer Res 5:208–215

Herfst LJ, Rook MB, Jongsma HJ (2004) Trafficking and functional expression of cardiac Na^+ channels. J Mol Cell Cardiol 36:185–193

Hirose M, Kuroda Y, Sawa S, Nakagawa T, Hirata M, Sakaguchi M, Tanaka Y (2004) Suppression of insulin signalling by a synthetic peptide KIFMK suggests the cytoplasmic linker between DIII-S6 and DIV-S1 as a local anaesthetic binding site on the sodium channel. Br J Pharmacol 142:222–228

Ishibashi H, Dinudom A, Harvey KF, Kumar S, Young JA, Cook DI (1999) Na^+ –H^+ exchange in salivary secretory cells is controlled by an intracellular Na^+ receptor. Proc Natl Acad Sci USA 96:9949–9953

Isom LL (2002) Beta subunits: players in neuronal hyperexcitability? Novartis Found Symp 241:124–138

Komada M, Soriano P (2002) BetaIV-spectrin regulates sodium channel clustering through ankyrin-G at axon initial segments and nodes of Ranvier. J Cell Biol 156:337–348

Kusaka S, Kapousta-Bruneau N, Green DG, Puro DG (1998) Serum-induced changes in the physiology of mammalian retinal glial cells: role of lysophosphatidic acid. J Physiol 506:445–458

Langley RR, Fidler IJ (2007) Tumor cell–organ microenvironment interactions in the pathogenesis of cancer metastasis. Endocr Rev 28:297–321

Laniado ME, Lalani EN, Fraser SP, Grimes JA, Bhangal G, Djamgoz MBA, Abel PD (1997) Expression and functional analysis of voltage-activated Na^+ channels in human prostate cancer cell lines and their contribution to invasion in vitro. Am J Pathol 150:1213–1221

Lee JH, Ryu IH, Kim EK, Lee JE, Hong S, Lee HK (2006) Induced expression of insulin-like growth factor-1 by amniotic membrane-conditioned medium in cultured human corneal epithelial cells. Invest Ophthalmol Vis Sci 47:864–872

Lemos VS, Poburko D, Chiu-Hsiang L, Cole WC, van Breemen C (2007) Na^+ entry via TRPC6 causes Ca^{2+} entry via NCX reversal in ATP stimulated smooth muscle cells. Biochem Biophys Res Commun 352:130–134

Liotta LA, Clair T (2000) Checkpoint for invasion. Nature 405:287–288

Liotta LA, Kohn EC (2001) The microenvironment of the tumour–host interface. Nature 411:375–379

Liu F, Verin AD, Borbiev T, Garcia JG (2001) Role of cAMP-dependent protein kinase A activity in endothelial cell cytoskeleton rearrangement. Am J Physiol 280:L1309–L1317

Malik-Hall M, Poon WY, Baker MD, Wood JN, Okuse K (2003) Sensory neuron proteins interact with the intracellular domains of sodium channel Nav1.8. Mol Brain Res 110:298–304

Melillo G, Semenza GL (2006) Exploiting the tumor microenvironment for therapeutics. Cancer Res 66:4558–4560

Mycielska ME, Djamgoz MBA (2004) Cellular mechanisms of direct-current electric field effects: galvanotaxis and metastatic disease. J Cell Sci 117:1631–1639

Nakamura T, Fidler IJ, Coombes KR (2007) Gene expression profile of metastatic human pancreatic cancer cells depends on the organ microenvironment. Cancer Res 67:139–148

Nilius B, Bohm T, Wohlrab W (1990) Properties of a potassium-selective ion channel in human melanoma cells. Pfluegers Arch 417:269–277

Onganer PU, Djamgoz MBA (2005) Small-cell lung cancer (human): potentiation of endocytic membrane activity by voltage-gated Na^+ channel expression in vitro. J Membr Biol 204:67–75

Onganer PU, Seckl MJ, Djamgoz MBA (2005) Neuronal characteristics of small-cell lung cancer. Br J Cancer 93:1197–1201

Ou Y, Strege P, Miller SM, Makielsski J, Ackerman M, Gibbons SJ, Farrugia G (2003) Syntrophin $\gamma 2$ regulates SCN5A gating by a PDZ domain-mediated interaction. J Biol Chem 278:1915–1923

Page MJ, Di Cera E (2006) Role of Na^+ and K^+ in enzyme function. Physiol Rev 86:1049–1092

Paget S (1889) The distribution of secondary growths in cancer of the breast. Lancet 1:571–573

Palmer CP, Mycielska ME, Burcu H, Osman K, Collins T, Beckerman R, Perrett R, Johnson H, Aydar E, Djamgoz MBA (2008) Single cell adhesion measuring apparatus (SCAMA): application to cancer cell lines of different metastatic potential and voltage-gated Na^+ channel expression. Eur Biophys J 37:359–368

Papa V, Milazzo G, Goldfine ID, Waldman FM, Vigneri R (1997) Sporadic amplification of the insulin receptor gene in human breast cancer. J Endocrinol Invest 20:531–536

Parrizas M, Gazit A, Levitzki A, Wertheimer E, LeRoith D (1997) Specific inhibition of insulin-like growth factor-1 and insulin receptor tyrosine kinase activity and biological function by tyrphostins. Endocrinology 138:1427–1433

Perks CM, Holly JM (2003) The insulin-like growth factor (IGF) family and breast cancer. Breast Dis 18:45–60

Postovit LM, Seftor EA, Seftor RE, Hendrix MJ (2006) Influence of the microenvironment on melanoma cell fate determination and phenotype. Cancer Res 66:7833–7836

Ratcliffe CF, Qu Y, McCormick KA, Tibbs VC, Dixon JE, Scheuer T, Catterall WA (2000) A sodium channel signaling complex: modulation by associated receptor protein tyrosine phosphatase beta. Nat Neurosci 3:437–444

Rodriguez-Pineiro AM, de la Cadena MP, Lopez-Saco A, Rodriguez-Berrocal FJ (2006) Differential expression of serum clusterin isoforms in colorectal cancer. Mol Cell Proteomics 5:1647–1657

Roger S, Besson P, Le Guennec J-Y (2003) Involvement of a novel fast inward sodium current in the invasion capacity of a breast cancer cell line. Biochim Biophys Acta 1616:107–111

Roger S, Rollin J, Barascu A, Besson P, Raynal PI, Iochmann S, Lei M, Bougnoux P, Gruel Y, Le Guennec J-Y (2007) Voltage-gated sodium channels potentiate the invasive capacities of human non-small-cell lung cancer cell lines. Int J Biochem Cell Biol 39:774–786

Snopko RM, Aromolaran AS, Karko KL, Ramos-Franco J, Blatter LA, Mejia-Alvarez R (2007) Cell culture modifies Ca^{2+} signalling during excitation–contraction coupling in neonate cardiac myocytes. Cell Calcium 41:13–25

Tas F, Duranyildiz D, Oguz H Camlica H, Yasasever V, Topuz E (2006) Serum vascular endothelial growth factor (VEGF) and interleukin-8 (IL-8) levels in small cell lung cancer. Cancer Invest 24:492–496

Tlsty TD, Coussens LM (2006) Tumor stroma and regulation of cancer development. Annu Rev Pathol 1:119–150

Tobe K, Asai S, Matuoka K, Yamamoto T, Chida K, Kaburagi Y, Akanuma Y, Kuroki T, Takenawa T, Kimura S, Nagai R, Kadowaki T (2003) Cystoskeletal reorganization induced by insulin: involvement of Grb2/Ash, Ras and phosphatidylinositol 3-kinase signaling. Genes Cells 8:29–40

Tysnes BB, Bjerkvig R (2007) Cancer initiation and progression: involvement of stem cells and the microenvironment. Biochim Biophys Acta 1775:283–297

van de Loosdrecht AA, Beelen RH, Ossenkoppele GJ, Broekhoven MG, Langenhuijsen MM (1994) A tetrazolium-based colorimetric MTT assay to quantitate human monocyte mediated cytotoxicity against leukemic cells from cell lines and patients with acute myeloid leukemia. J Immunol Methods 174:311–320

Wada A, Yanagita T, Yokoo H, Kobayashi H (2004) Regulation of cell surface expression of voltage-dependent Nav1.7 sodium channels: mRNA stability and posttranscriptional control in adrenal chromaffin cells. Front Biosci 9:1954–1966

Weigelt B, Peterse JL, van 't Veer LJ (2005) Breast cancer metastasis: markers and models. Nat Rev Cancer 5:591–602

Witz IP, Levy-Nissenbaum O (2006) The tumor microenvironment in the post-PAGET era. Cancer Lett 242:1–10

Yamamoto R, Yanagita T, Kobayashi H, Yuhi T, Yokoo H, Wada A (1996) Up-regulation of functional voltage-dependent sodium channels by insulin in cultured bovine adrenal chromaffin cells. J Neurochem 67:1401–1408

Yoshida Y, Tsuzuki K, Ishiuchi S, Ozawa S (2006) Serum-dependence of AMPA receptor-mediated proliferation in glioma cells. Pathol Int 56:262–271

Zebedin E, Mille M, Speiser M, Zarrabi T, Sandtner W, Latzenhofer B, Todt H, Hilber K (2007) C_2C_{12} skeletal muscle cells adopt cardiac-like sodium current properties in a cardiac cell microenvironment. Am J Physiol 292:H439–H450

Zhang H, Yee D (2004) The therapeutic potential of agents targeting the type 1 insulin-like growth factor receptor. Expert Opin Investig Drugs 13:569–577

Zhang H, Polzer AM, Kiang DT, Yee D (2007) Down-regulation of type 1 insulin-like growth factor receptor increase sensitivity of breast cancer cells to insulin. Cancer Res 67(1):391–397